Coexistence of the 1q and 2q incommensurate phases and memory effect in barium sodium niobate

J. M. Kiat
Laboratoire de Chimie-Physique du Solide, Ecole Centrale, 92295 Chatenay-Malabry, France and Laboratoire Léon Brillouin, Commissariat à l'Énergie Atomique-Centre National de la Recherche Scientifique, CEN-Saclay 91191 Gif sur Yvette, France

G. Calvarin
Laboratoire de Chimie-Physique du Solide, Ecole Centrale, 92295 Chatenay-Malabry, France

J. Schneck
Centre National d'Etudes des Télécommunications 92200 Bagneux, France
(Received 13 May 1993)

Using high-resolution x-ray diffraction on single crystals we specify the phase diagram of barium sodium niobate between 20 and 300 °C. Its main characteristics are the coexistence of two incommensurate phases in the vicinity of the normal-incommensurate transition, a $2q$ tetragonal phase and a $1q$ orthorhombic phase, and a progressive $2q/1q$ transformation in the temperature range where a large thermal hysteresis of the misfit parameter is observed. A complex memory effect is evidenced when the sample is annealed inside the incommensurate phases or the quasicommensurate phase: a pinning of the modulation on a very large plateau of temperature and a delay or an anticipation of the $2q/1q$ transformation and of the lock-in transition is evidenced. We discuss our results on the basis of the $2q/1q$ phase coexistence and the existence of mobile effects in the structure of barium sodium niobate (sodium vacancies) interacting with the modulations.

I. INTRODUCTION

Nonstandard incommensurate behaviors with a large amplitude have been widely reported in insulator barium sodium niobate (B.S.N.).[1] In particular, a large thermal hysteresis in the temperature dependence of the misfit parameter δ, of the integrated intensity and of the full width at half maximum (FWHM) of satellite peaks, as well as in other physical quantities such as optical birefringence Δn, have been evidenced in the temperature range of the incommensurate orthorhombic phase ($T_L \simeq 260$ °C, $T_I \simeq 305$ °C). In addition, it was observed that a residual incommensurability persists at $T < T_L$ in the so-called quasicommensurate phase where the δ parameter remains at a quasiconstant value of the order of 1% a^*. This peculiar $\delta = f(T)$ evolution is also characterized by a strong discontinuous jump ($\simeq 10\%$) at the lock-in temperature T_L when heating from room temperature, whereas a continuous decrease is observed when cooling from the normal high-temperature phase.

Some characteristics of B.S.N., such as the values of temperatures T_L and T_I or the existence of another phase transition at low temperature (at about 110 K) depend on the exact composition of the crystal:[2] indeed there is usually a nonstoichiometry in single crystals of B.S.N., whose structural consequence is the existence of sodium vacancies, which should be able to diffuse throughout the sample.[3] This is why, among different hypotheses, which can *a priori* explain these nonstandard behaviors (intrinsic pinning on the lattice, fixed, or mobile defect effects), the role of the mobile vacancies was particularly considered.

The disclosure of a slow relaxation with time in the line shape of the incommensurate satellite peaks[4] and in the optical birefringence,[5] when the sample is annealed at a temperature T_R within the incommensurate phase, as well as the large modifications in the subsequent evolution of δ and $\Delta n = f(T)$, seemed to confirm the importance of mobile defects. As a matter of fact, most of the latter results could be discussed in the framework of the memory effect,[6] specific to incommensurate systems, whose basic assumption is an interaction between mobile defects and the incommensurate modulation leading to an ordered pattern of these defects (defect density wave or DDW).

However, high-resolution x-ray-diffraction experiments[7] have revealed a more complex situation than a "simple" memory effect, i.e., a splitting of the modulation into two components when the temperature is lowered after an annealing at T_R, and a specific temperature dependence of the ferroelastic pattern which has been related to the behavior of the modulation. On the basis of these results an inhomogeneous state constituted by the coexistence of two incommensurate phases was conjectured. Further confirmations of this hypothesis came from a combination of x-ray, optical, and TEM measurements as well as theoretical considerations.[8–14] It was shown that B.S.N. exhibits a coexistence of an orthorhombic phase with a single direction of modulation ($1q$ state, previously considered alone) and a tetragonal phase

with two perpendicular directions of modulation ($2q$ state). The appearance of the $2q$ phase during a thermal cycling coincides with the transformation of large ferroelastic domains into microdomains.[12]

The purpose of this article is to specify the characteristics of both these phases, their respective range of stability in temperature and the consequences of an annealing on their relative stability. In particular, we show that the large thermal hysteresis of the misfit parameter and its complex memory effect are directly connected to the coexistence of the $2q$ and $1q$ phases.

The paper is organized as follows. In Sec. II experimental information on the x-ray measurements are given. In Sec. III some characteristics of the two incommensurate phases are described, both their basic lattices and their modulation vectors, and their relative stability versus temperature are discussed. We emphasize the existence of a $2q/1q$ transformation whose kinetic is described in Sec. IV. The consequences of an annealing on the modulation vectors and on the lattices are presented in Sec. V, as well as the induced changes in the stability of both phases. These results are globally discussed in Sec. VI on the basis of the $2q/1q$ coexistence and of the interaction modulations—defects.

II. EXPERIMENTAL

Bragg and satellite reflections of a single crystal were recorded on a prototype high-resolution two axis diffractometer previously described[15] with a collimated Cu $K\alpha$ radiation issued from an 18 kW rotating anode. In standard conditions the instrumental width is about $33\times10^{-3^\circ}$ θ for $\theta=50°$. In order to obtain a higher resolution a backward planar monochromator (001 of an InP plane single crystal) was used in certain cases. This setup allowed us to minimize the widening due to the spectral distribution of the radiation: for instance, the FWHM of the Bragg peak 1800 of B.S.N. was divided by more than a factor of 4 ($9\times10^{-3^\circ}$ θ against $33\times10^{-3^\circ}$ θ) when using the 006 reflection of the InP monochromator. Heating of the samples was achieved through a high-temperature attachment Huber 231. The temperature was controlled within 0.5° and the thermal gradient in the probed region of the crystal had a maximal value of 2°.

The investigated sample has a nominal composition $Ba_{2.11}Na_{0.84}Nb_{4.99}O_{15}$.[2] The average symmetry at room temperature is $Bbm2$ and the lattice parameters are $a=17.5958$ Å, $b=17.6326$ Å, and $c=7.9938$ Å. Single crystals with typical sizes of $0.4\times0.4\times4$ mm were oriented on the diffractometer in order to study the orthorhombic reciprocal planes (a^*,c^*) (Fig. 1) which includes main Bragg reflections with h and l even and related satellite peaks through the vector of modulation $\mathbf{Q}=[(1+\delta)\mathbf{a}^*/2+\mathbf{c}^*]$. For instance, the Bragg peak 1800 has two first-order satellite peaks $18+(1+\delta)/201$ and $18-(1+\delta)/201$.

As the room-temperature orthorhombic symmetry results from a breaking of the tetragonal symmetry at the normal-incommensurate transition ($T=T_I$), two kinds of ferroelastic domains (corresponding to an exchange of a and b) can be simultaneously observed in the probed area.

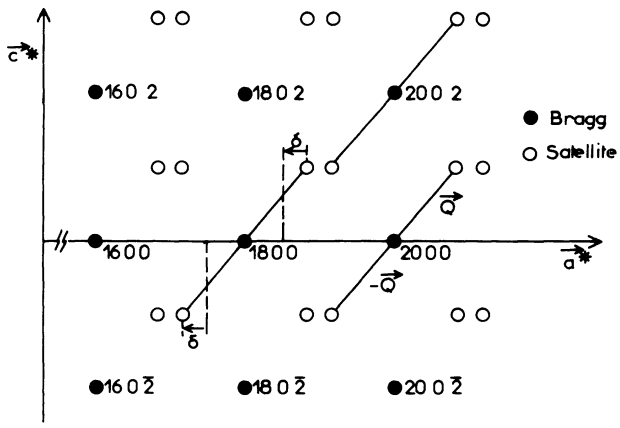

FIG. 1. Schematic representation of a part of the $h\,0\,l$ reciprocal plane, which includes main Bragg reflections and their related satellite peaks.

Recordings of the doublet $h\,0\,0$ and $0\,h\,0$ allowed us to measure the cell parameters a and b, their associated lengths of coherence, and the relative volumic ratio of each state. During this work we have mainly performed $\theta-2\theta$ scans on the 1800, 0 180, and 2000, 0200 Bragg doublets, and on the $18+(1+\delta)/201$, $19-(1+\delta)/201$, and $20+(1+\delta)/201$ satellite peaks. Such high values of indices of reflection were chosen in order to obtain a high precision in the cell and misfit parameters, as well as to have directions of $\theta-2\theta$ scans nearly parallel to a^*; for instance, the angle between the a^* and the scan direction is for the $20+(1+\delta)/201$ satellite peak 6.1° at room temperature.

III. PHASE DIAGRAM OF B.S.N. BETWEEN 20 AND 300 °C

A. Experimental results

In previous papers[8,9] we have shown that within a certain range of temperature the $2q$ phase could be detected in x-ray experiments by the appearance of a supplementary Bragg peak besides the usual Bragg doublet characteristic of the orthorhombic symmetry. This supplementary reflection has been associated with the occurrence of a new phase with an average tetragonal symmetry and a characteristic cell parameter a' with a value between those of the two orthorhombic parameters a and b. Similarly, in the same temperature range, long exposure precession photographs revealed weak $2q$ satellite spots in the b^* direction perpendicularly to that of the orthorhombic $1q$ direction of modulation a^*[9]. The second set of $2q$ satellite spots, equivalent by the fourfold axis, is superimposed to the $1q$ ones because their respective incommensurate misfit parameters are (within the precision of the measurement) equal. These $2q$ satellite peaks are too weak to be evidenced by the goniometric method using during the present experiments; only the contribution of the $1q$ satellites could be probed.

In order to specify the properties and the respective

range of stability of the $1q$ and $2q$ phases the Bragg and satellite peaks were scanned repetitively during thermal cyclings (2.5°/min) from room temperature up to the normal phase, then back again to room temperature. This thermal cycling reference procedure was adopted because the ranges of stability of both incommensurate phases are deeply modified by the memory effect and thus by the thermal history of the samples, as will be shown later in this paper.

The temperature evolution between 20 and 350°C, both in heating and cooling, of the profiles of the orthorhombic doublet 1800 and 0180 is presented in Fig. 2. The temperature dependence of the cell parameters a, b ($1q$ orthorhombic phase), and a' ($2q$ tetragonal phase), of the misfit parameter δ, of the intensity and of the FWHM of the $20+(1+\delta)/201$ satellite peak are respectively given in Figs. 3–5.

At room temperature, the cell is orthorhombic and the observed doublet corresponds to the parameters a and b, with the greater volumic fraction corresponding to the a orientation of ferroelastic domains. The misfit parameter is weak, $\delta=1.2\%$, but nonzero: it is the so-called $1q$ quasicommensurate phase. An anisotropic widening of the satellite reflections is disclosed, as compared to the Bragg ones: in the direction of modulation a^* the deconvoluted width of the satellites is about 1.5 greater than the corresponding Bragg peaks which are almost resolution limited. In the c^* direction both the satellite and Bragg peaks have the same width.

When heating, only a slight decrease of the orthorhombic distortion is observed up to about 230°C (Figs. 2 and 3). In this temperature region the intensity of the "a peak" decreases whereas its width increases. At $T_L=260$°C a supplementary a' peak is detected; its FWHM is equivalent to those of the a and b peaks in the quasicommensurate phase. At T_L, the misfit parameter also displays an abrupt jump up to 8.7% (Fig. 4) and an

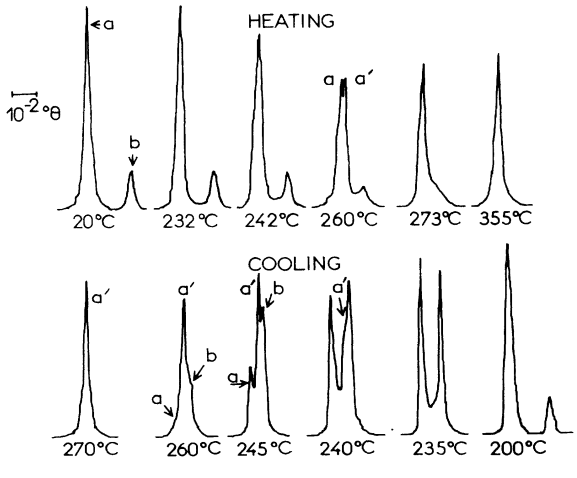

FIG. 2. Experimental profiles of the orthorhombic doublet 1800 and 0180 (a and b peaks) and of the corresponding a' tetragonal peak for some temperatures both on heating and cooling runs (between 245 and 235°C on cooling the intensities have been enlarged by a factor of about 3).

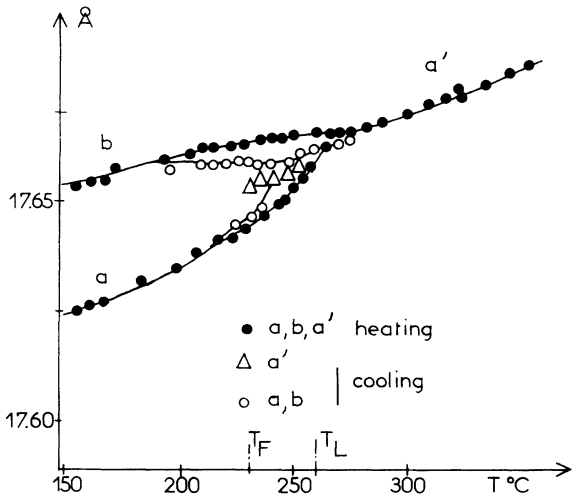

FIG. 3. Temperature dependence of cell parameters a, b ($1q$ orthorhombic phase), and a' ($2q$ tetragonal phase).

important increase of the FWHM of satellite peaks along a^* is observed (Fig. 5): the width of the incommensurate peak just above T_L is 2.4 greater than its room-temperature value and remains constant up to T_I. By contrast, its integrated intensity decreases continuously. Above T_L the intensity of the a and b peaks and the corresponding orthorhombic distortion b-a are so weak that they only contribute to the foot of the Bragg peak which is now essentially the a' peak; this resultant peak becomes progressively resolution limited as the temperature increases from T_L. In the temperature range T_L-T_I δ increases almost linearly up to 12% (Fig. 4). Above T_I

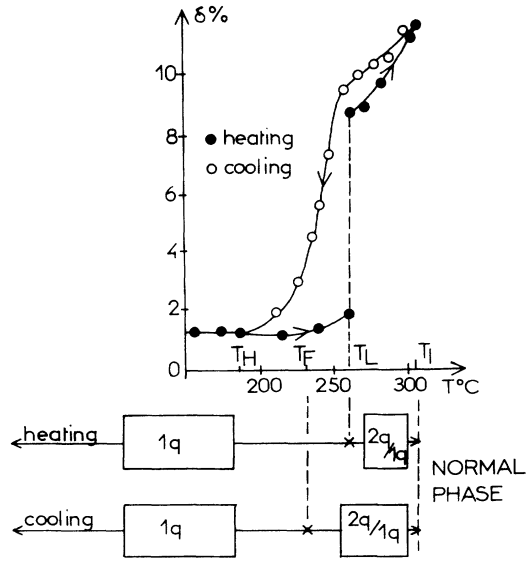

FIG. 4. Phase diagram of B.S.N.: the temperature dependence of the misfit parameter δ of the $1q$ phase is plotted with a schematic representation of the single state $1q$ or the two states $2q/1q$, depending on the temperature range.

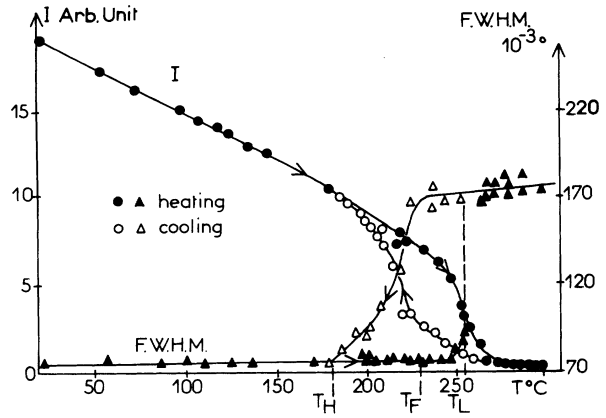

FIG. 5. Temperature dependence of the integrated intensity and of the FWHM of the satellite peak $20+(1+\delta)/201$.

the satellite peak has vanished and only one Bragg peak corresponding to the high-temperature tetragonal phase is observed with a FWHM equivalent to that of the orthorhombic peaks at room temperature.

When cooling from the normal phase the same phenomena are qualitatively observed with a thermal hysteresis. Down to about 270 °C ($T_L+10°$) the Bragg peak is essentially the a' peak and its profile remains almost unchanged; at this temperature, the misfit parameter decreases linearly with a weak thermal hysteresis. Below this later temperature the intensity of the a' peak starts to decrease and its width starts to increase, particularly at the base of the peak (a and b-peaks contribution). These phenomena occur progressively down to T_L. Below T_L the intensity of the a peak increases to the detriment of the a' peak: at 245 °C ($T_L-15°$) for instance, the three components a, a', and b are clearly separated (Fig. 2). At 235 °C the a' peak has almost disappeared and below 230 °C (the temperature is called T_F after this) it has completely vanished: the same profile as during the heating run is recovered. Also, below T_L, the thermal evolution of the misfit parameter and of the FWHM of satellite peaks displays a rapid but continuous decreasing; compared with the heating run a large thermal hysteresis is then observed. Both heating and cooling curves connect together at $T_H=180$ °C, the temperature below which the quasicommensurate state is recovered (Fig. 4).

B. Phase diagram

The respective range of stability of both incommensurate phases can be deduced from the evolutions of the $1q$ satellite peak, a and b orthorhombic Bragg peaks, and $2q$ tetragonal Bragg a' peak. The different characteristic temperatures are dependent on the cooling and heating rate; moreover, they also depend slightly on the value of the nonstoichiometry of the samples (sodium vacancies). However, the main characteristics are always observed whatever the temperature rate of variation and whatever the composition of the samples; these characteristics are (i) the coexistence inside the incommensurate phase of a $1q$ orthorhombic phase with a $2q$ tetragonal phase and (ii) the transformation on cooling of the $2q$ phase into the $1q$ phase inside the temperature range of the thermal hysteresis of the misfit parameter, with a large phase coexistence during this transition; on heating the $1q$ phase transforms into the $2q$ phase, but this transformation is not complete as the two phases coexist up to T_I.

Two or three main regions of this so-called phase diagram (although not in equilibrium conditions) must be respectively considered during the heating or cooling run.

1. Heating run

From room temperature up to T_L the $1q$ orthorhombic quasicommensurate phase is observed alone. At T_L the misfit parameter displays a discontinuous jump: it is the lock-in transition. Similarly, the $1q$ phase transforms into the $2q$ tetragonal phase (whose signature is the a' peak) in a temperature range of about 10°. However, the transformation is not complete and the $1q$ satellite peak is still detected up to T_I. So the coexistence of both $2q$ and $1q$ incommensurate phases is observed between T_L and T_I. Above T_I the normal tetragonal phase is recovered.

2. Cooling run

When cooling from the normal tetragonal phase the coexistence of the $2q$ and $1q$ phase is evidenced just below T_I by the observation of the Bragg a' peak and of the $1q$ satellite peak. The intensity of this satellite peak does not change when cycling through T_I; this indicates that the volumic ratio of both phases just below T_I is a constant of the sample (this point will be more strongly demonstrated in Sec. V A 2). On further cooling the $2q$ phase begins to transform into the $1q$ phase at a temperature of about $T_L+10°$ (270 °C) and has completely disappeared at $T_F\simeq 230$ °C. Similarly, the lock-in of the $1q$ misfit parameter occurs; that is, the δ misfit parameter value gradually decreases. However, in contrast to the heating run no discontinuity in the δ thermal evolution could be detected. Below T_F the crystal is single phased ($1q$ state) still with a high δ value (about 4%) which continuously decreases on further cooling; at a temperature $T_H\simeq 180$ °C the quasicommensurate phase is recovered.

IV. KINETIC OF THE $2q$ /$1q$ TRANSFORMATION

As previously indicated all the experiments described in the last section were performed using a thermal cycling reference procedure of 2.5°/min. However, if the thermal run is interrupted inside the incommensurate phase a time dependence of the characteristics of the Bragg peak is observed (Fig. 6) which corresponds to (i) a decrease of the a'-peak intensity and an increase of the a-peak intensity, (ii) a small increase of the b-a orthorhombic distortion, and (iii) an increase of the FWHM of the a'-peak and a decrease of the FWHM of the a peak.

Similarly, a time dependence of the line shape of the incommensurate satellite peaks occurs. It consists of an increase of their integrated intensity associated to a narrowing with time of their FWHM (these later observa-

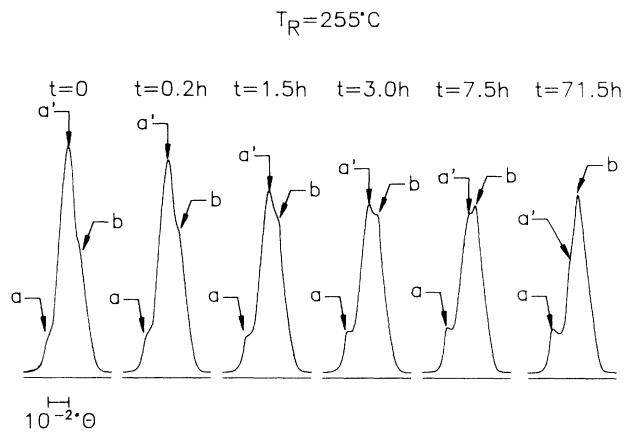

FIG. 6. Time dependence of the line shape of a Bragg peak during an annealing in the incommensurate phases at $T_R = 255\,°C$.

tions have already been reported[4]). Moreover, a small decrease of the misfit parameter is evidenced (Fig. 7). All these effects have a maximum amplitude at the T_L temperature.

On the other hand, no time dependence of the line shape of satellite and Bragg peaks is observed during annealing inside the quasicommensurate phase ($T < T_H$ on cooling curve, $T < T_L$ on heating curve), nor for Bragg peaks inside the normal phase ($T > T_I$).

The time dependence of the satellite peak characteristics was previously interpreted[4] as a consequence of an interaction between the modulation and the mobile defects. However, our present observations show that both the Bragg and the satellite reflections have the same time dependence characteristics (i.e., several hours) within the same temperature range (i.e., in the $2q/1q$ range of coexistence). So these time dependences are more likely to be associated with the existence of a kinetic of the $2q/1q$ transformation, the evolution of the satellite intensity being a consequence of the increase with time of the volume of the $1q$ phase and the effect on the width being associated to the increase of the length of coherence of this phase.

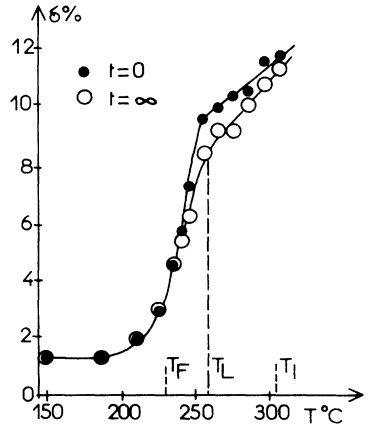

FIG. 7. δ misfit parameter value at the beginning and the end of annealings on the cooling curve.

V. STABILITY OF THE $2q/1q$ PHASES AND MEMORY EFFECT

The results described in this section show that an annealing at $T = T_R$ in the incommensurate phase or in the quasicommensurate phase induces changes of the relative stability of the $2q$ and $1q$ phases, depending on the temperature range of T_R. The main result is that the thermal evolution of both lattice and modulation characteristics (cell parameters, modulation vectors, relative ratio of the $2q/1q$ phases, and their respective lengths of coherence) differs considerably from the nonannealed case. On the other hand, after an annealing inside the normal phase ($T_R > T_I$) no change of these characteristics is observed; so in the following paragraphs we only discuss the $T_R < T_I$ cases. As the observed behaviors are complex we discuss separately for the purpose of clarity the subsequent cooling and heating runs performed after the annealing at T_R.

A. Thermal evolution of the $2q$ and $1q$ phases after an annealing inside the incommensurate phase

1. *Cooling run after annealing*

In the first stage of the experiments the crystal is cooled from the normal phase inside the incommensurate phase ($T_H < T_R < T_I$) at a rate of 2.5°/min and maintained at a given temperature T_R. Then, when the characteristics of both the lattice and satellite peaks have reached their saturation values with time, i.e., after several days (Sec. IV) the peaks are scanned during a cooling run from T_R down to room temperature, always at 2.5°/min. The thermal evolution of the misfit parameters are shown in Fig. 8 for some typical temperatures T_R; they are to be compared with the nonannealed case of Fig. 4.

Different effects could be observed depending on the value of T_R.

(i) If $T_H < T_R < T_F$ [Fig. 8(a)] the sample is single phased ($1q$ phase); the thermal evolution of the modulation displays a plateau down to room temperature. The misfit parameter (hereafter called δ_F) and the associated FWHM of the satellite peak remain pinned to their value at T_R so that the system remains in a $1q$ incommensurate state down to room temperature.

(ii) If $T_F < T_R < T_L$ [Fig. 8(b)] the sample is in a state corresponding to the mixing of the $2q$ and $1q$ phases. The volumic fraction of each phase can be deduced from the intensity of the a' peak with respect to that of the a and b peaks. When cooling from T_R to a temperature T_{L1} depending on T_R, the volumic fraction of the $2q$ and $1q$ phases remains pinned, on a large temperature range, to the value measured at the end of the annealing at T_R. Similarly, the FWHM of the Bragg peaks respectively associated to these two phases also remains pinned to the

T_R value. However, the orthorhombic distortion associated with the $1q$ phase increases when the temperature is decreased from T_R. Consequently, the three components a, b, and a' peaks constituting the Bragg profile are clearly resolved in a large range of temperature between T_R and T_{L1}. Below T_{L1} a progressive vanishing of the a' peak is observed whereas the intensity of the a peak increases. These phenomena are associated to the transformation of the $2q$ tetragonal part of the sample into the orthorhombic $1q$ phase.

The position and the FWHM of the incommensurate satellite peak are also pinned between T_R and T_{L1}, resulting in the occurrence of a quasiplateau of δ_F at its T_R value. At T_{L1} the transition $2q/1q$ does not affect this satellite peak and the plateau of δ_F is observed down to room temperature. The main effect occurring below T_{L1} is the progressive growth to a second satellite peak with a quasicommensurate misfit parameter $\delta_f < 1\%$ which coexists with the δ_F component. Thus, below T_{L1} and down to room temperature, the sample is in a $1q$ phase but with two very different states of modulations: an incommensurate state and a quasicommensurate state respectively associated to the δ_F and δ_f satellite peaks (the corresponding satellite peak is in the inset of Fig. 8).

(iii) If $T_R > T_L$ [Figs. 8(c) and 8(d)] the pinning of the $2q/1q$ phase coexistence and a plateau of modulation δ_F are also observed down to T_{L1}. At T_{L1} a second δ_f satellite peak still appears but with a higher value of misfit parameter than in the previous case $T_F < T_R < T_L$: the higher T_R is, the higher δ_f is [Fig. 8(d)]. Parallely the $2q/1q$ transformation takes place. Below T_{L1} this δ_f component decreases continuously and pins at a T_{L2} temperature to a weak quasicommensurate value ($< 1\%$). At this very temperature the quasiplateau of δ_F is interrupted by a transition where the satellite δ_F disappears and locks discontinuously at a low quasicommensurate value $\delta_{f'}$ very close to the δ_f one. So below T_{L2} the sample is in a $1q$ phase with two very similar quasicommensurate states of modulation associated to the $\delta_{f'}$ and δ_f satellite peaks.

Thus, when a crystal is cooled from the normal phase and maintained for several days inside the incommensurate phase at a temperature T_R, a further cooling down to room temperature can lead to a very different situation from that of a nonannealed crystal.

(a) If $T_H < T_R < T_F$ one single incommensurate component of modulation (δ_F) is observed between T_R and room temperature.

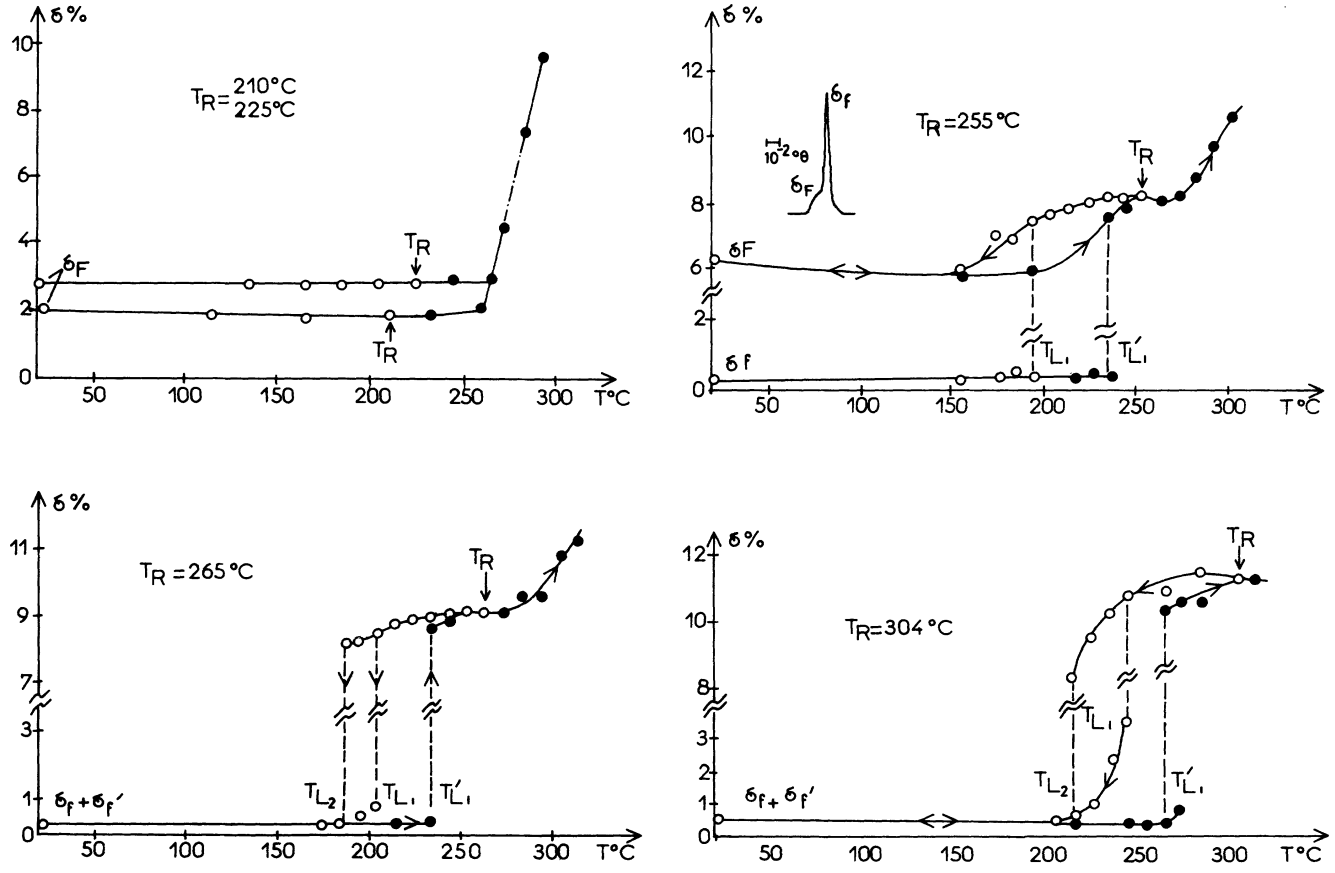

FIG. 8. Thermal evolution of the misfit parameters on cooling down to room temperature and subsequent heating after an annealing at T_R. (a) $T_H < T_R < T_F$: annealings in a single $1q$ incommensurate state; (b) $T_F < T_R < T_L$: annealing in a two $2q/1q$ incommensurate state; the inset shows a rocking curve at room temperature of the corresponding satellite peaks; (c) and (d) $T_R > T_L$: same as (b) but at higher temperatures.

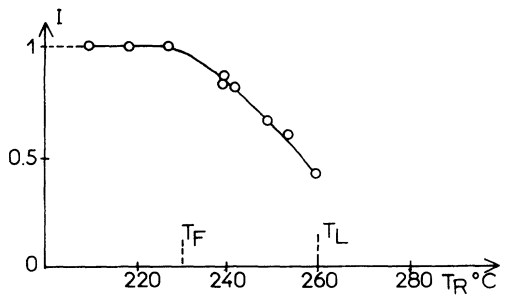

FIG. 9. Relative intensity I of the satellite peak associated with the δ_F component at room temperature for different annealing temperatures T_R; $I=I\delta_F/(I\delta_F+I\delta_f)$.

(b) If $T_F<T_R<T_L$ one component of modulation with a high value of misfit parameter δ_F is observed between T_R and room temperature in addition with one quasicommensurate component δ_f, which is observed below T_{L1}. Their relative intensity $I=I\delta_F/(I\delta_F+I\delta_f)$ at room temperature depends on T_R: the weaker I is, the higher T_R is (Fig. 9).

(c) If $T_R>T_L$ one quasicommensurate component δ_f is observed below T_{L1} and one quasicommensurate component $\delta_{f'}$ is observed below T_{L2} with very close values and in a relative intensity which seems to be T_R independent.

2. *Subsequent heating run from room temperature*

When the sample is cooled down to room temperature after an annealing at T_R the thermal evolutions which are observed during a subsequent heating run are very different from those of a nonannealed crystal.

(i) If $T_H<T_R<T_F$ [Fig. 8(a)], at room temperature a component with a high value of incommensurability δ_F is observed; when heating, the same plateaus of δ_F and FWHM are observed on the heating run compared to the cooling run.

(ii) If $T_F<T_R<T_L$ [Fig. 8(b)], at room temperature a component with a high value of incommensurability δ_F coexists with a quasicommensurate peak δ_f; when heating, an hysteresis is observed in the δ_F evolution whose extension is increasing with T_R. The thermal evolution of the δ_f peak also displays an hysteresis increasing with T_R: the associated satellite peak vanishes at a $T_{L'1}$ temperature higher than T_{L1} but always lower than the T_L temperature of a nonannealed sample.

(iii) If $T_R>T_L$ [Figs. 8(c) and 8(d)], at room temperature two components with weak values of incommensurability (δ_f and $\delta_{f'}$) coexist; when heating, the component (with quasicommensurate value) $\delta_{f'}$ transforms into the incommensurate δ_F component at a temperature close to $T_{L'1}$ whereas the δ_f component displays an hysteresis and vanishes at a $T_{L'1}$ temperature higher than T_{L1} but always lower than T_L.

In all these experiments, when heating from room temperature, the appearance of the $1q/2q$ transformation is detected by the observation of the a peak at the very temperature where the δ_f component vanishes (i.e., $T_{L'1}$). When the temperature T_R is crossed on the heating run a single satellite peak δ_F with the same characteristics as at the end of the annealing is recovered and the same Bragg peak profile is recovered.

Above T_R a plateau is observed in the δ_F misfit parameter and the associated FWHM evolution for several tenths of degrees, as well as a pinning of the volumic ratio of the $1q/2q$ phases. Beyond, the nonannealed characteristics are recovered. The precise determination of the new normal-incommensurate transition temperature T_I is difficult because of the weak intensity of satellite peaks, but for $T_R>T_L$ an increase of about 10° could be evidenced. All the effects observed on the heating run above T_R can also be observed if the heating run is performed directly after the annealing.

B. Thermal evolution of the modulation after an annealing inside the quasicommensurate phase or inside the normal phase

As previously mentioned, no time dependence of satellite and Bragg peaks is observed when an annealing is performed inside the quasicommensurate phase (i.e., for $T_R<T_H$ on the cooling curve, or $T_R<T_L$ on the heating curve). However, a very different behavior is observed in the subsequent thermal cyclings. If the sample is heated (directly from T_R or after cooling down to room temperature) it remains in the quasicommensurate state (characterized by a low value of the misfit parameter and of FWHM) even above T_L, which is the lock-in temperature of a nonannealed sample. In fact, after such an annealing the lock-in temperature is delayed to a higher temperature $T_{L'1}$. The closer T_R is to T_L, the higher $T_{L'1}$ is: for instance, an annealing performed on the heating curve at $T_R=T_L-1°$ leads to a very large delay of the lock-in at $T_{L'1}=T_L+40°$. Moreover, the a' peak appears on heating at the very temperature $T_{L'1}$. On the other hand, if a sample is annealed in the normal phase ($T_R>T_I$) no difference of behavior for the modulation nor for the $2q/1q$ state could be detected in the subsequent thermal cycling.

C. Summary

An annealing can have the following drastic effects both on the lattices and on modulations.

(i) An annealing inside the incommensurate phase can pin the volumic proportion of the $1q/2q$ phases for several tens of degrees when cooling or heating from T_R, leading respectively to a delay or an anticipating in the critical temperature of the $1q/2q$ transformation. Compared with a nonannealed sample the $2q$ phase is then stabilized on cooling with regard to the $1q$ phase, whereas an annealing in the quasicommensurate phase stabilizes the $1q$ phase on heating compared to the $2q$ phase.

(ii) Parallel to the pinning of the $1q/2q$ volumic ratio, a large quasiplateau of the δ_F modulations and of associated FWHM of satellite peaks is observed. The transformation of the $2q$ phase into the $1q$ phase when cooling has for consequence the appearance of a lower incom-

mensurability δ_f while the component δ_F is still observed. Further cooling induces the lock-in of the $1q$ phase (transition $\delta_F/\delta_{f'}$) at a temperature lower than that of an nonannealed crystal. On the other hand, an annealing inside the quasicommensurate phase leads to a large increase of the lock-in transition temperature.

(iii) Moreover, all the modifications previously described which are induced by an annealing inside the incommensurate or quasicommensurate phase are erased if an annealing is performed afterward inside the normal phase.

VI. DISCUSSION

A. Interpretation of the experiments

Some of the effects described in the preceding section are typical of what has been called the memory effect in incommensurate systems. They are the possibility to pin over a large range of temperature the incommensurate misfit parameter at any value realized in the incommensurate phase, the anticipating or delaying of the lock-in transition, and the possibility to erase these effects at will.

Similar effects with much smaller amplitudes have already been reported in some insulating compounds (Thiourea, Rb_2ZnCl_4...) and in some charge density wave compounds.[6,16] They have been interpreted in assuming the existence in the structure of mobile defects which can diffuse under the action of the modulation; as a consequence, an annealing inside the incommensurate phase leads to an ordered pattern of defects with the same periodicity than that of the modulation (defect density wave or DDW). When the temperature is rapidly changed (i.e., with respect to the ordering time of the defects) this DDW remains present inside the sample and tends to lock the modulation to its periodicity. During further thermal cyclings there is a competition between three states: the incommensurate state, the commensurate state, and the state which satisfies the underlying potential of the DDW. When this latter potential is prominent, the modulation is pinned on a plateau, whereas when the lock-in potential, on cooling, or the incommensurate potential, on heating, become the strongest the modulation reaches its nonannealed value. The existence of this defect potential leads to an anticipation of the lock-in transition on further heating from the commensurate phase.

More complex phenomena, both on lattices and modulations are observed in B.S.N. in relation to the coexistence of the $2q/1q$ phases: in addition to the pinning of modulations, a delay or an anticipating of the $2q/1q$ transformation is observed when the sample is annealed inside the incommensurate phase or the quasicommensurate phase.

The $2q/1q$ coexistence was theoretically discussed on the basis of a soliton structure for the $2q$ phase.[17] In this framework, the $2q$ soliton structure can be built up by the juxtaposition of commensurate domains of the $1q$ phase with an ordered pattern such that the average tetragonal symmetry is recovered. Consequently, the $2q/1q$ phase coexistence observed in our x-ray experiments is related to the existence of domains having different sizes: the $1q$ phase corresponding to large orthorhombic domains (typical size larger than the x-ray coherence length) and the $2q$ phase corresponding to an ordered pattern of small $1q$ orthorhombic domains (the typical size is smaller than the x-ray coherence length). However, up to now this model had received no experimental support.

The experiments described above supports this physical picture of the $2q/1q$ phase coexistence. Indeed, in this model, the pinning of the $2q$ solitons (which are the ferroelastic walls of the $1q$ phase) should result in modifications of the stability of both $2q$ and $1q$ phases in addition to the pinning of modulations. Hereafter we discuss our results on the basis of the existence of mobile defects (sodium vacancies) in the structure of B.S.N., which interact with the modulations (solitons) inside the $1q/2q$ phases. Thus the physical picture of the memory effect in B.S.N. is the creation of two different systems of DDW during an annealing. The underlying idea for the interpretation of the different effects observed is a competition of two defect potentials with the incommensurate and the lock-in potentials.

1. *Annealing inside the incommensurate state*

The interpretation of pinnings of the δ_F modulation down to room temperature observed after an annealing at low-temperature ($T_H < T_R < T_F$) where the sample is in a single $1q$ phase is straightforward: in these cases we deal with a "simple and classical" memory effect of an incommensurate phase. On the other hand, for $T_R > T_F$ special attention is required because the sample is in a two phase $1q/2q$ state. The pinning of the modulations induces (on cooling) the plateau of the δ_F parameter as well as the pinning of volumic proportion of both phases down to T_{L1}. At T_{L1} the $2q$ phase is unpinned first and the $2q/1q$ transition occurs. Below this temperature the crystal is in a $1q$ single-phase state with two very different misfit parameters: the quasicommensurate δ_f value associated to the $1q$ phase resulting from the transformation of the $2q$ phase, and the high incommensurate δ_F parameter still pinned, associated to the $1q$ phase already present before the $2q/1q$ transformation. For annealings below the lock-in temperature ($T_R < T_L$) the pinning of the modulation δ_F is strong enough to induce a plateau extending down to room temperature, whereas for annealings above T_L the lock-in of the δ_F parameter is observed at a temperature T_{L2}.

If the sample is heated afterwards, the persistence of the DDW results in the anticipation of the $1q/2q$ and lock-in transitions at a temperature $T_{L'1}$ lower than that of a nonannealed sample (T_L). Above this $T_{L'1}$ temperature the pinning of the modulations on the DDW is recovered and induces a plateau above T_R. At higher temperatures the influence of the DDW is no more prominent and the nonannealed behavior is recovered.

2. *Annealing inside the quasicommensurate phase*

In these cases ($T_R < T_H$ on the cooling run, or $T_R < T_L$ on the heating run) we deal again with a classical memory

effect: the pinning of the quasicommensurate modulation retains the single-phase $1q$ above T_L on heating; the $1q/2q$ and lock-in transitions occur at a higher temperature $T_{L'1}$.

The delaying and anticipation of the $2q/1q$ and lock-in transitions is the memory effect specific to B.S.N. This effect (as well as the kinetic effects described in Sec. IV) is stronger for annealings in the vicinity of the lock-in temperature T_L where the anharmonicity of modulations is supposed to be the strongest. In the normal phase the DDW's are destroyed by thermal diffusion of the defects and the memory effect is erased.

B. Experimental verification of the model

In the framework of the mechanism proposed above, the appearance of the quasicommensurate component of modulation δ_f below T_{L1} on cooling after an annealing is related to the $2q/1q$ transition, more precisely to the appearance of the $1q$ phase corresponding to the transformation of the $2q$ phase. Thus the relative volume τ of the $1q$ phase which appears below T_{L1} should be evaluated by two independent methods. First, it can be deduced from the change of relative intensity of the Bragg a peak:

$$\tau=[Ia(T)-Ia(T_R)]/I_{\text{tot}} .$$

Second, it must be equal to the relative integrated intensity of the δ_f satellite peak: $\tau=I_{\delta f}/I_{\text{tot}}$ (I_{tot} is the total intensity of the Bragg or satellite peak, respectively). Through a fitting program for diffraction experiments we have plotted the value of τ deduced from Bragg and satellite peaks during the cooling run after an annealing at $T_R=255\,^{\circ}\text{C}$ (Fig. 10). A good agreement between both types of measurements is achieved. Between T_R and T_{L1} the $2q/1q$ transformation is delayed and no supplementary $1q$ phase appears, so $\tau=0$; at T_{L1} the $2q/1q$ transformation begins and is achieved at T_{L2} when all the $2q$ phase is transformed into the $1q$ phase.

Thus, the constant value τ for $T<T_{L2}$ is a measure-

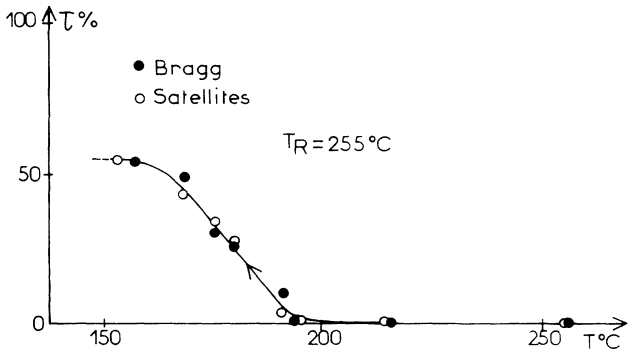

FIG. 10. Relative volume τ of the $1q$ phase which appears below T_{L1} after an annealing at a temperature $T_R=255\,^{\circ}\text{C}$. τ is deduced from the change of intensity of the Bragg a peak: $\tau=[Ia(T)-Ia(T_R)]/I_{\text{tot}}$ and from the relative integrated intensity of the δ_f satellite peak: $\tau=I\delta_f/I_{\text{tot}}$ (I_{tot} is the total intensity of the Bragg and satellite peak, respectively).

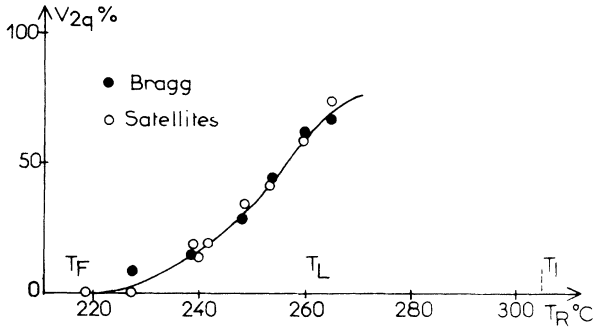

FIG. 11. Relative volume V_{2q} of the $2q$ phase observed at the end of different annealing at T_R temperatures, deduced from Bragg and satellite peak measurements.

ment of the relative volume of the $1q$ phase at the end of the annealing at T_R, when the modulations and the mobile defects are in equilibrium. We have plotted in Fig. 11 the quantity $V_{2q}=1-\tau$, which gives the relative volume of the $2q$ phase, deduced from similar curves to Fig. 10 for various annealing temperatures. Above about T_L+10° we were not able to precisely measure the V_{2q} value but it has reached the limiting value which is a constant of each sample: in the analyzed sample there is about 80% of the volume which is in the $2q$ phase at high temperature. At lower temperature the $2q/1q$ transformation begins in the vicinity of $T_L=260\,^{\circ}\text{C}$ and ends at $T_F=220\,^{\circ}\text{C}$; below this temperature the sample is $1q$ single phased.

VII. CONCLUSION

Using high-resolution x-ray diffraction on both Bragg and satellite peaks we have clarified the phase diagram of B.S.N. At high temperature the crystal is in a $2q/1q$ two-phase state. When cooling a progressive transformation of the $2q$ phase into the $1q$ phase occurs. Similarly, there is a continuous lock-in of the modulation vectors to their quasicommensurate value. When heating from room temperature the $1q/2q$ transformation is abrupt and the lock-in is discontinuous.

Annealings inside the incommensurate phase have shown the possibility of delaying the lock-in and $2q/1q$ transitions for several tenths of degrees: the $2q$ phase is then stabilized against the $1q$ phase on cooling, whereas an annealing inside the quasicommensurate phase stabilizes the $1q$ phase on heating. These phenomenon reveal a complex memory effect which results from the interaction of mobile defects with the $1q$ and $2q$ modulations in soliton structures.

The large thermal hysteresis in the evolution of the misfit parameter δ in a nonannealed sample is then to be associated to the $2q/1q$ coexistence and not to the effect of defects as previously assumed. However, our results show that these defects can deeply change the behavior of the modulations if they are left to diffuse inside the structure. In this framework, the puzzling difference between the heating and cooling curve of the $\delta=f(T)$ (discontinuous or continuous lock-in transition) could be associ-

ated to the difficulty for the 1q phase to nucleate inside the 2q phase on cooling, leading to a continuous 2q/1q transition. However, much work is still needed to clarify this problem.

ACKNOWLEDGMENTS

Laboratoire de Chemie-Physique du solide is Unité de Recherche Associée au CNRS No. 453.

[1]J. C. Toledano, J. Schneck, and G. Errandonéa, *Incommensurate Phases in Dielectrics, Modern Problems in Condensed Matter Sciences* (North-Holland, Amsterdam, 1985), Vol. 14-2, p. 233.

[2]J. Schneck, Thèse de doctorat d'état, Université de Paris VI, 1982.

[3]J. Dolinsek, R. Blinc, and J. Schneck, Solid State Commun. **70**, 1077 (1989).

[4]J. Schneck, G. Calvarin, and J. M. Kiat, Phys. Rev. B **29**, 3 (1984); **29**, 1476 (1984).

[5]G. Errandonéa, J. C. Tolédano, A. Litzler, H. Savary, J. Schneck, and J. Aubrée, J. Phys. (Paris) Lett. **45**, L329 (1984).

[6]P. Lederer, G. Montambaux, J. P. Jamet, and M. Chauvin, J. Phys. (Paris) Lett. **45**, L627 (1984); P. Jamet and P. Lederer, *ibid.* **44**, L257 (1983).

[7]J. M. Kiat, G. Calvarin, and J. Schneck, Jpn. J. Appl. Phys. **24**, 2 (1985); **24**, 832 (1985).

[8]J. M. Kiat, G. Calvarin, and J. Schneck, Ferroelectrics **105**, 219 (1990); J. M. Kiat, Thèse de doctorat d'état, Université de Paris VI, 1988.

[9]J. Schneck, J. C. Toledano, G. Errandonea, A. Litzler, H. Savary, C. Manolikas, J. M. Kiat, and G. Calvarin, Phase Trans. **9**, 359 (1987).

[10]C. Manolikas, J. Schneck, J. C. Toledano, J. M. Kiat, and G. Calvarin, Phys. Rev. B **35**, 8884 (1987).

[11]S. Barre, H. Mutka, and C. Roucau, Phys. Rev. B **38**, 9113 (1988).

[12]P. X. Qing, H. M. Shen, Y. M. Hui, and F. Duan, Phys. Status Solidi (a) **92**, 57 (1985).

[13]J. M. Kiat, Y. Uesu, M. Akutsu, and J. Aubréee, Ferroelectrics **125**, 227 (1992).

[14]W. F. Oliver, J. F. Scott, S. A. Lee, and S. M. Lindsay, J. Phys. Condens. Matter **2**, 10 (1990); **2**, 2465 (1990).

[15]J. F. Berar, G. Calvarin, and D. Weigel, J. Appl. Crystallogr. **14**, 149 (1980).

[16]*Incommensurate Phases in Dielectrics, Modern Problems in Condensed Matter Sciences,* edited by R. Blinc and A. P. Levanyuk (North-Holland, Amsterdam, 1985).

[17]J. C. Toledano (private communication).